closely related to SHs; they are small and similar in size,[28,30] and both express CYP3A1 and 2E1 at a low level.[28,32] At 3 weeks posttransplantation, the CFPHs were small in size, had a large nucleus-to-cytoplasm ratio, and expressed hCD44, but not hCK19. At 10 weeks, the cells became bigger, assumed a morphology similar to that of PH-derived cells, and lost their expression of hCD44. The expression of hCYP3A4 was quite low (0.15-fold) among CFPHs compared with that of PHs (data not shown). In addition, the distribution of hCYP3A4-expressing CFPHs in the pericentral zone was unique: more than two-thirds of CFPHs did not express CYP3A4. In the case of the h-PH–chimeric mice, all PHs in the pericentral zone expressed CYP3A4 (data not shown).

Presently, we lack experimental data to explain the expression of hCYP3A4 in CFPH-chimeric liver, but CFPHs may require some specific environmental factor(s) for differentiation, which might be absent from mouse liver. Alternatively, some factors that specifically inhibit the differentiation of CFPHs might be present there. CK7-positive h-hepatic progenitor cells are present in the livers of uPA/SCID mice transplanted with h-postnatal liver-derived PHs,[6] and these small cells are strongly immunoreactive to pan-cytokeratin with scant cytoplasm. The CFPHs were morphologically similar to these cells at 3 weeks posttransplantation, although we were unable to detect CK7-positive cells in either the PH- or CFPH-transplanted chimeric livers. However, CFPHs were hCK7-, hCK19-, and hCD44-positive, at least until 1 day posttransplantation (data not shown).

We reported previously that uPA/SCID livers were nearly completely replaced with young donor PHs at 10 weeks posttransplantation.[5] In contrast, the RIs of our CFPH-chimeric mice were <30% at 9 to 10 weeks. CFPHs were rare in the host liver at 3 weeks posttransplantation, whereas several PHs were observed. The lower RIs of the CFPHs might be attributable to their lower engraftment efficiency.

In conclusion, h-hepatocytes in immunodeficient, and liver-injured mice are useful for the study of viral hepatitis. Repopulated h-hepatocytes are susceptible to infection with HBV[6-8] and HCV.[4,6] Additionally, h-hepatocyte–chimeric mice are usually produced by transplanting fresh[6,7] or cryopreserved hepatocytes,[4,5] but sources of h-hepatocytes are limited. Several studies have reported on liver repopulation by in vitro–propagated cells from adult and fetal livers, such as immortalized mouse hepatic stem cells,[29] rat SHPCs,[34] immortalized h-hepatocytes transfected with full-length HBV,[35] and fetal h-epithelial/hepatic progenitor cells.[36,37] However, the RIs in these studies were extremely low (less than a few percent). In the present

study, we were able to produce CFPH-chimeric mice with RIs as high as 27%. Thus, CFPHs could be an alternative to h-hepatocytes as a source of hepatocytes for transplantation. Moreover, the CFPH-chimeric mice were susceptible to infection with HBV, even though their serum hALB levels were extremely low (10^2-10^3 ng/mL). CFPH-chimeric mice will be useful for studying h-HBV and for characterizing h-hepatic progenitor cells.

References

1. Rhim JA, Sandgren EP, Degen JL, Palmiter RD, Brinster RL. Replacement of diseased mouse liver by hepatic cell transplantation. Science 1994; 263:1149-1152.
2. Overturf K, Al-Dhalimy M, Ou CN, Finegold M, Grompe M. Serial transplantation reveals the stem-cell-like regenerative potential of adult mouse hepatocytes. Am J Pathol 1997;151:1273-1280.
3. Laconi E, Oren R, Mukhopadhyay DK, Hurston E, Laconi S, Pani P, et al. Long-term, near-total liver replacement by transplantation of isolated hepatocytes in rats treated with retrorsine. Am J Pathol 1998;153:319-329.
4. Mercer DF, Schiller DE, Elliott JF, Douglas DN, Hao C, Rinfret A, et al. Hepatitis C virus replication in mice with chimeric human livers. Nat Med 2001;7:927-933.
5. Tateno C, Yoshizane Y, Saito N, Kataoka M, Utoh R, Yamasaki C, et al. Near completely humanized liver in mice shows human-type metabolic responses to drugs. Am J Pathol 2004;165:901-912.
6. Meuleman P, Libbrecht L, De Vos R, de Hemptinne B, Gevaert K, Vandekerckhove J, et al. Morphological and biochemical characterization of a human liver in a uPA-SCID mouse chimera. HEPATOLOGY 2005;41: 847-856.
7. Dandri M, Burda MR, Török E, Pollok JM, Iwanska A, Sommer G, et al. Repopulation of mouse liver with human hepatocytes and in vivo infection with hepatitis B virus. HEPATOLOGY 2001;33:981-988.
8. Tsuge M, Hiraga N, Takaishi H, Noguchi C, Oga H, Imamura M, et al. Infection of human hepatocyte chimeric mouse with genetically engineered hepatitis B virus. HEPATOLOGY 2005;42:1046-1054.
9. Kocarek TA, Schuetz EG, Guzelian PS. Biphasic regulation of cytochrome P450 2B1/2 mRNA expression by dexamethasone in primary cultures of adult rat hepatocytes maintained on matrigel. Biochem Pharmacol 1994; 48:1815-1822.
10. Arterburn LM, Zurlo J, Yager JD, Overton RM, Heifetz AH. A morphological study of differentiated hepatocytes in vitro. HEPATOLOGY 1995;22: 175-187.
11. Tateno C, Yoshizato K. Growth and differentiation in culture of clonogenic hepatocytes that express both phenotypes of hepatocytes and biliary epithelial cells. Am J Pathol 1996;149:1593-1605.
12. Tateno C, Takai-Kajihara K, Yamasaki C, Sato H, Yoshizato K. Heterogeneity of growth potential of adult rat hepatocytes in vitro. HEPATOLOGY 2000;31:65-74.
13. Yamasaki C, Tateno C, Aratani A, Ohnishi C, Katayama S, Kohashi T, et al. Growth and differentiation of colony-forming human hepatocytes in vitro. J Hepatol 2006;44:749-757.
14. Hino H, Tateno C, Sato H, Yamasaki C, Katayama S, Kohashi T, et al. A long-term culture of human hepatocytes which show a high growth poten-

tial and express their differentiated phenotypes. Biochem Biophys Res Commun 1999;256:184-191.

15. Kocken, JM, de Heer E, Borel Rinkes IH, Sinaasappel M, Terpstra OT, Bruijn JA. Blocking of $\alpha 1\beta 1$ integrin strongly improves survival of hepatocytes in allogeneic transplantation. Lab Invest 1997;77:19-28.

16. Prall F, Nollau P, Neumaier M, Haubeck HD, Drzeniek Z, Helmchen U, et al. CD66a (BGP), an adhesion molecule of the carcinoembryonic antigen family, is expressed in epithelium, endothelium, and myeloid cells in a wide range of normal human tissues. J Histochem Cytochem 1996;44:35-41.

17. Kon J, Ooe H, Oshima H, Kikkawa Y, Mitaka T. Expression of CD44 in rat hepatic progenitor cells. J Hepatol 2006;45:90-98.

18. Yovchev MI, Grozdanov PN, Joseph B, Gupta S, Dabeva MD. Novel hepatic progenitor cell surface markers in the adult rat liver. HEPATOLOGY 2007;45:139-149.

19. Rippin SJ, Hagenbuch B, Meier PJ, Stieger B. Cholestatic expression pattern of sinusoidal and canalicular organic anion transport systems in primary cultured rat hepatocytes. HEPATOLOGY 2001;33:776-782.

20. Sandgren EP, Palmiter RD, Heckel JL, Daugherty CC, Brinster RL, Degen JL. Complete hepatic regeneration after somatic deletion of an albumin-plasminogen activator transgene. Cell 1991;66:245-256.

21. Oinonen T, Lindros KO. Hormonal regulation of the zonated expression of cytochrome P-450 3A in rat liver. Biochem J 1995;309:55-61.

22. Sonnier M, Cresteil T. Delayed ontogenesis of CYP1A2 in the human liver. Eur J Biochem 1998;251:893-898.

23. Sell S. Is there a liver stem cell? Cancer Res 1990;50:3811-3815.

24. Thorgeirsson SS. Hepatic stem cells. Am J Pathol 1993;142:1331-1333.

25. Shafritz DA, Oertel M, Menthena A, Nierhoff D, Dabeva MD. Liver stem cells and prospects for liver reconstitution by transplanted cells. HEPATOLOGY 2006;43(Suppl):89S-98S.

26. Masson NM, Currie IS, Terrace JD, Garden OJ, Parks RW, Ross JA. Hepatic progenitor cells in human fetal liver express the oval cell marker Thy-1. Am J Physiol Gastrointest Liver Physiol 2006;291:G45-G54.

27. Petersen BE, Goff JP, Greenberger JS, Michalopoulos GK. Hepatic oval cells express the hematopoietic stem cell marker Thy-1 in the rat. HEPATOLOGY 1998;27:433-445.

28. Gordon GJ, Coleman WB, Grisham JW. Temporal analysis of hepatocyte differentiation by small hepatocyte-like progenitor cells during liver regeneration in retrorsine-exposed rats. Am J Pathol 2000;157:771-786.

29. Strick-Marchand H, Morosan S, Charneau P, Kremsdorf D, Weiss MC. Bipotential mouse embryonic liver stem cell lines contribute to liver regeneration and differentiate as bile ducts and hepatocytes. Proc Natl Acad Sci U S A 2004;101:8360-8365.

30. Katayama S, Tateno C, Asahara T, Yoshizato K. Size-dependent *in vivo* growth potential of adult rat hepatocytes. Am J Pathol 2001;158:97-105.

31. Mitaka T, Mikami M, Sattler GL, Pitot HC, Mochizuki Y. Small cell colonies appear in the primary culture of adult rat hepatocytes in the presence of nicotinamide and epidermal growth factor. HEPATOLOGY 1992;16:440-447.

32. Asahina K, Shiokawa M, Ueki T, Yamasaki C, Aratani A, Tateno C, et al. Multiplicative mononuclear small hepatocytes in adult rat liver: their isolation as a homogeneous population and localization to periportal zone. Biochem Biophys Res Commun 2006;342:1160-1167.

33. Yoshizato K. Growth potential of adult hepatocytes in mammals: highly replicative small hepatocytes with liver progenitor-like traits. Dev Growth Differ 2007;49:171-184.

34. Gordon GJ, Butz GM, Grisham JW, Coleman WB. Isolation, short-term culture, and transplantation of small hepatocyte-like progenitor cells from retrorsine-exposed rats. Transplantation 2002;73:1236-1243.

35. Brown JJ, Parashar B, Moshage H, Tanaka KE, Engelhardt D, Rabbani E, et al. A long-term hepatitis B viremia model generated by transplanting nontumorigenic immortalized human hepatocytes in Rag-2-deficient mice. HEPATOLOGY 2000;31:173-181.

36. Malhi H, Irani AN, Gagandeep S, Gupta S. Isolation of human progenitor liver epithelial cells with extensive replication capacity and differentiation into mature hepatocytes. J Cell Sci 2002;115:2679-2688.

37. Nowak G, Ericzon BG, Nava S, Jaksch M, Westgren M, Sumitran-Holgersson S. Identification of expandable human hepatic progenitors which differentiate into mature hepatic cells *in vivo*. Gut 2005;54:972-979.

Differential MicroRNA Expression Between Hepatitis B and Hepatitis C Leading Disease Progression to Hepatocellular Carcinoma

Shunsuke Ura,[1] Masao Honda,[1,2] Taro Yamashita,[1] Teruyuki Ueda,[1] Hajime Takatori,[1] Ryuhei Nishino,[1] Hajime Sunakozaka,[1] Yoshio Sakai,[1] Katsuhisa Horimoto,[3] and Shuichi Kaneko[1]

MicroRNA (miRNA) plays an important role in the pathology of various diseases, including infection and cancer. Using real-time polymerase chain reaction, we measured the expression of 188 miRNAs in liver tissues obtained from 12 patients with hepatitis B virus (HBV)-related hepatocellular carcinoma (HCC) and 14 patients with hepatitis C virus (HCV)-related HCC, including background liver tissues and normal liver tissues obtained from nine patients. Global gene expression in the same tissues was analyzed via complementary DNA microarray to examine whether the differentially expressed miRNAs could regulate their target genes. Detailed analysis of the differentially expressed miRNA revealed two types of miRNA, one associated with HBV and HCV infections (n = 19), the other with the stage of liver disease (n = 31). Pathway analysis of targeted genes using infection-associated miRNAs revealed that the pathways related to cell death, DNA damage, recombination, and signal transduction were activated in HBV-infected liver, and those related to immune response, antigen presentation, cell cycle, proteasome, and lipid metabolism were activated in HCV-infected liver. The differences in the expression of infection-associated miRNAs in the liver correlated significantly with those observed in Huh7.5 cells in which infectious HBV or HCV clones replicated. Out of the 31 miRNAs associated with disease state, 17 were down-regulated in HCC, which up-regulated cancer-associated pathways such as cell cycle, adhesion, proteolysis, transcription, and translation; 6 miRNAs were up-regulated in HCC, which down-regulated anti-tumor immune response. *Conclusion:* miRNAs are important mediators of HBV and HCV infection as well as liver disease progression, and therefore could be potential therapeutic target molecules. (HEPATOLOGY 2009;49:000-000.)

MicroRNA (miRNA) is an endogenous, small, single-strand, noncording RNA consisting of 20 to 25 bases and regulates gene expression of various cell types. It plays an important role in various biological processes, including organ development and differentiation as well as cellular death and proliferation, and is also involved in various diseases such as infection and cancer.[1-3]

miRNAs are produced as follows. A primary miRNA with a hairpin loop structure is cleaved into a precursor miRNA and transported out of the nuclei with a carrier protein (Exportin-5). The precursor miRNA is then processed by Dicer and converted into an active single-strand RNA in the cytoplasm. The miRNA binds to a target messenger RNA in a sequence-dependent manner and induces degradation of the target messenger RNA and translational inhibition. One miRNA regulates the expression of multiple target genes; bioinformatics analyses have suggested that the expression of more than 30% of human genes is regulated by miRNAs.[4-7]

1

Infection of the human liver with hepatitis B virus (HBV) and hepatitis C virus (HCV) induces the development of chronic hepatitis (CH), cirrhosis, and in some instances hepatocellular carcinoma (HCC).[8] The virological features of these two distinct viruses are completely different; however, the viruses infect the liver and cause CH, which is not distinguished by histological examination or clinical manifestations. We previously reported that gene expression profiles in chronic hepatitis B (CH-B) and chronic hepatitis C (CH-C) are different. Proapoptotic and DNA repair responses were predominant in CH-B, and inflammatory and antiapoptotic phenotypes were predominant in CH-C. However, factors inducing these differences in gene expression remain to be elucidated.[9,10]

We examined miRNA expression in liver tissue with HBV-related liver disease (CH-B and HCC-B) and HCV-related liver disease (CH-C and HCC-C) and in normal liver tissue via real-time detection polymerase chain reaction (RTD-PCR). We also performed global analysis of messenger RNA expression in these tissues using complementary DNA (cDNA) microarray. These analyses allowed us to find characteristic miRNAs associated with HBV or HCV infection as well as the progression of liver disease.

Materials and Methods

Patients. The study subjects included 12 patients with CH-B complicated by HCC and 14 patients with CH-C complicated by HCC. Gene expression analysis was approved by the ethics committee of the Graduate School of Medicine, Kanazawa University Hospital, Japan, between 1999 and 2004. In addition, nine normal liver tissue samples obtained during surgery for metastatic liver cancer were used as control samples. Surgically removed liver tissues were stored in liquid nitrogen until analysis. Histological classification of HCC and histological evaluation of hepatitis in noncancerous regions for each patient are shown in Table 1. HCV viremia in two patients with CH-C was persistently cleared by interferon therapy before HCC development. There were no significant differences in the histological findings of HCC and noncancerous regions, as well as in sex, age, and hepatic function between the HBV and HCV infection groups.

Quantitative RTD-PCR. Approximately 1 mg of each liver tissue sample stored in liquid nitrogen was ground with a homogenizer while still frozen, and total RNA containing miRNA was isolated according to the protocol of the mirVana miRNA Isolation kit (Ambion, Austin, TX) and stored at −80°C until analysis. miRNA expression levels were quantitated using the TaqMan MicroRNA Assays Human Panel Early Access kit (Applied Biosystems, Foster City, CA). cDNA was prepared via reverse transcription using 10 ng each of the isolated total RNA and 3 μL each of the reverse transcription primers with specific loop structures. Reverse transcription was performed using the TaqMan MicroRNA Reverse Transcription kit (Applied Biosystems) according to the manufacturer's protocol. Then, a mixture of 6.67 μL of nuclease-free water, 10 μL of TaqMan 2 × Universal PCR Master Mix (No AmpErase UNG; Applied Biosystems), and 2 μL of TaqMan MicroRNA Assay Mix, which was included in the kit, was prepared for each sample on a 384-well plate; 1.33 μL of the reverse transcription product was added to the mixture, and amplification reaction was performed on an ABI PRISM 7900HT (Applied Biosystems). Expression levels of 188 miRNAs in each sample were quantitated.

Analysis of RTD-PCR Data. The measured 188 miRNAs included RNU6B, which is commonly used as a control for miRNA. β-Actin and glyceraldehyde 3-phosphate dehydrogenase were also measured simultaneously for correcting RNA amount. The mean Ct values and standard deviations of each miRNA were calculated from expression data of all patients obtained by RTD-PCR. miRNA with the lowest expression variation was used as the internal control. Ct values of each miRNA were then corrected by the Ct value of the internal control to yield −ΔCt values defined as relative miRNA expression levels and used for analyses. Statistical analyses and hierarchical cluster analyses of expression data were performed using BRB ArrayTools (http://linus.nci.nih.gov/BRB-Array-Tools.html). Relative miRNA expression levels were further normalized using the median over the all patients so that the normalized expression levels of each patient have a median log ratio of 0. A class prediction method was used for classifying two patient groups based on the supervised learning method, and a binary tree classification method was used for classifying three or more patient groups with a statistical algorithm of the support vector machine (SVM). Class prediction was performed using SVM incorporating genes differentially expressed at a univariate parametric significance level of $P = 0.01$. The prediction rate was estimated via cross-validation and the bootstrap method for small sample data.[11] (It is worth noting that the prediction rate may be likely an overestimate of the true rate, given the weaknesses of cross-validation and bootstrapping methods in a strict sense.)

Microarray Analysis. cDNA microarray slides (Liver chip 10k) were used as described.[10] RNA isolation, amplification of antisense RNA, labeling, and hybridization were performed according to the protocols described.[9,10] Quantitative assessment of the signals on the slides was

Table 1. Characteristics of Patients Used for Analysis of miRNA and Microarray Samples

Patient No.	Virus	Age	Sex	ALT	Histology of Activity	Background Liver Fibrosis	Histological Grade of HCC	Tumor Size (mm)	TNM Staging	HCV-RNA (KIU/mL)	HBV-DNA (LEG/mL)
1	HBV	57	M	16	2	4	Moderate	20	II	−	3.4
2	HBV	51	M	57	1	2	Moderate	48	II	−	< 2.6
3	HBV	61	M	17	1	4	Well	16	II	−	< 3.7
4	HBV	47	M	19	1	4	Moderate	15	I	−	< 3.7
5	HBV	72	M	19	1	1	Well	25	II	−	NA
6	HBV	73	M	62	1	3	Moderate	45	III	−	5.7
7	HBV	42	M	36	1	4	Moderate	18	I	−	< 3.7
8	HBV	63	M	13	1	2	Moderate	15	I	−	2.8
9	HBV	68	F	54	1	2	Well	56	II	−	4.1
10	HBV	70	M	13	0	2	Well	40	II	−	< 3.7
11	HBV	58	M	29	1	4	Moderate	35	IVA*	−	3.3
12	HBV	72	M	22	1	4	Moderate	18	I	−	6
13	HCV	66	F	33	2	4	Well	25	II	423	−
14	HCV	67	M	89	1	4	Well	30	II	> 850	−
15	HCV	64	M	31	1	4	Moderate	75	III	< 5 (+)	−
16	HCV	68	M	30	0	4	Well	23	II	> 850	−
17	HCV	46	M	98	2	3	Moderate	20	I	> 850	−
18	HCV	68	F	32	2	4	Moderate	25	III	< 5 (+)	−
19	HCV	66	F	46	2	4	Well	25	II	> 850	−
20	HCV	47	M	246	1	3	Moderate	20	I	262	−
21	HCV	75	M	27	1	3	Moderate	19	II	85.1	−
22	HCV	77	M	21	0	1	Moderate	20	II	< 5 (−)	−
23	HCV	66	M	46	2	2	Well	60	II	50.3	−
24	HCV	65	M	89	1	1	Poorly	25	III	850	−
25	HCV	53	M	54	0	1	Moderate	28	II	< 5 (−)	−
26	HCV	75	F	212	1	4	Well	19	I	580	−
27	−	51	F	18	0	0	−	−	−	−	−
28	−	78	F	13	0	0	−	−	−	−	−
29	−	75	M	20	0	0	−	−	−	−	−
30	−	34	M	12	0	0	−	−	−	−	−
31	−	64	M	30	0	0	−	−	−	−	−
32	−	78	M	9	0	0	−	−	−	−	−
33	−	53	M	19	0	0	−	−	−	−	−
34	−	64	F	12	0	0	−	−	−	−	−
35	−	60	F	20	0	0	−	−	−	−	−

HCV RNA was assayed via Amplicor Monitor Test (KIU/mL); HBV DNA was assayed via transcription-mediated amplification (LEG/mL).

Abbreviations: ALT, alanine aminotransferase; F, female; HBV, hepatitis B virus; HCC, hepatocellular carcinoma; HCV, hepatitis C virus; M, male; TNM, tumor-node-metastasis.

*Vascular invasion (+).

performed by scanning on the ScanArray 5000 (General Scanning, Watertown, MA) followed by image analysis using GenePix Pro 4.1 (Axon Instruments, Union City, CA) as described.[10]

Preliminary Survey of Independency of Paired Samples from the Same Patient. CH and HCC expression data were derived from the same patient. Before further analysis, we examined whether the miRNA expression of paired samples was similar or independent. We compared differences in the expressions of paired and nonpaired CH and HCC samples using the Dunnett test[12] (Supplementary Data). All possible tests performed for data pairs represented no dependency due to the paired data from the same patients. For data analysis, we used the standard pairwise class comparison and prediction tool in BRB ArrayTools.

Identification of Candidate miRNA Target Genes. Candidate target genes predicted to be regulated by miRNAs based on sequence comparison were selected using MIRANDA Pro3.0 (Sanger Institute). Of the selected genes, those represented on a microarray chip were then examined for expression (Fig. 4). The number of genes showing a significant ($P <0.05$) expression difference among the candidate target genes represented on the chip was statistically analyzed to evaluate the significance of expression regulation by miRNAs. Analysis of significance was performed using Hotelling T2 test (BRB ArrayTools).

Pathway Analysis. Of the candidate miRNA target genes, those showing a significant ($P < 0.01$) expression difference between N, CH-B, HCC-B, CH-C, and HCC-C samples were analyzed for pathways involving
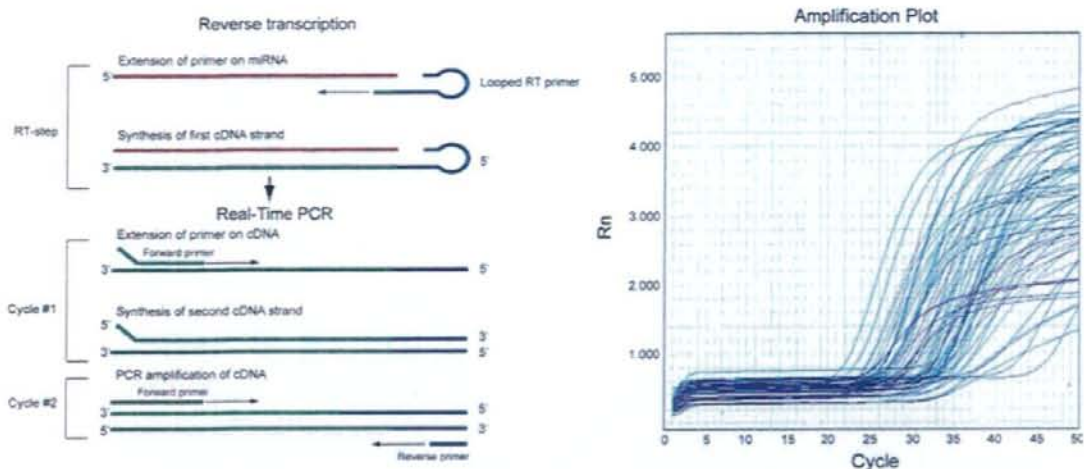
Fig. 1. (A) miRNA-specific RTD-PCR using sheet hairpin primers. (B) miRNA amplification curves by RTD-PCR.

these genes using MetaCore software suite (GeneGo, St. Joseph, MI). Significance probability was calculated using the hypergeometrical distribution based on gene ontology terms. Because one gene is frequently involved in multiple pathways, all pathways corresponding to the genes with significance probability were listed.

Verification of Regulation of Candidate Target Genes by miRNAs. Small interfering RNAs (Ambion) specific to 13 miRNAs (has-miR-17*, has-miR-20a, has-miR-23a, has-miR-26a, has-miR-27a, has-miR-29c, has-miR-30a, has-miR-92, has-miR-126, has-miR-139, has-miR-187, has-miR-200a, and has-miR-223) showing significant differences in expression were transfected into Huh7 cells using TransMessenger transfection reagent (QIAGEN, Valencia, CA), and loss of function of each miRNA was evaluated. Similarly, precursor miRNAs of five miRNAs (has-miR-23a, has-miR-26a, has-miR-27a, has-miR-92, and has-miR-200a) were also transfected into Huh7 cells, and gain of function of each miRNA was evaluated. The loss- and gain-of-function of miRNAs were evaluated via RTD-PCR. In addition, different gene expressions regulated by miRNAs were also evaluated via RTD-PCR.

HBV/HCV Infection Model Using Cultured Cells. The plasmid pHBV 1.2 coding the 1.2-fold length of the HBV genome was transfected into Huh7.5 cells using Fugene6 transfection reagent (Roche Applied Science, Indianapolis, IN). HBeAg production in culture medium was measured using Immunis HBeAg/Ab EIA (Institute of Immunology Co., Ltd., Tokyo, Japan).[13] The amount of HBV-DNA was measured via RTD-PCR (Supplementary Fig. 1A,B). JFH1-RNA was transfected into Huh7.5 cells using TransMessenger transfection reagent (QIA-

GEN) and the expression of the core protein was examined via immunofluorescence staining using anti-HCV core antibody (Affinity BioReagent, CO).[14,15] HCV-RNA amount was also measured via RTD-PCR (Supplementary Fig. 1A,B). JFH1/GND was used as a negative control. miRNA expression was quantitated by RTD-PCR 48 hours after transfection.

Results

Expression of miRNA in Liver Tissue. A panel of miRNA was successfully amplified from liver tissues via RTD-PCR. The representative amplification profile of miRNA as determined with RTD-PCR is shown in Fig. 1. To assess the reliability and reproducibility of this assay system, we first measured RNU6B in duplicate from all samples in different plates. The mean difference in Ct values of RNU6B expression within the same samples was 0.08 ± 0.05 (mean $\pm$ standard deviation), indicating the high reproducibility of this assay. All Ct values from each reaction were collected, and Ct variation obtained by each probe from all patients was calculated. Although RNU6B was frequently used as the internal control, the standard Ct variation was relatively high (Ct, 27 ± 1.94), suggesting that the variances in its value depend on the state of liver disease (N, CH and HCC). Therefore, we selected has-miR-328 as the internal control with the smallest standard deviation (Ct, 30 ± 0.60). The relative expression ratio of individual miRNA to has-miR-328 was calculated and applied to the following analysis using a BRB-array tool.

Hierarchical cluster analysis revealed that the expression profiles of the 188 miRNAs from each patient were

A

B
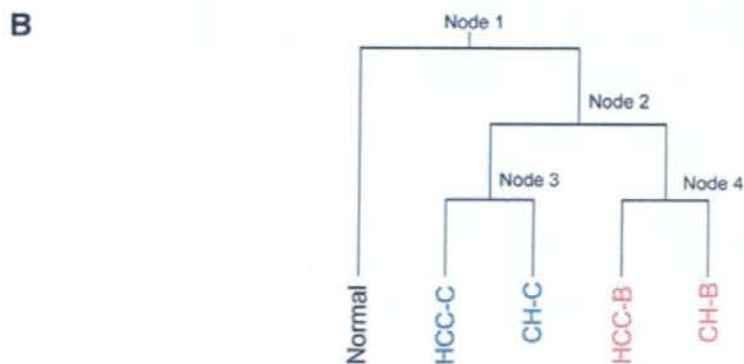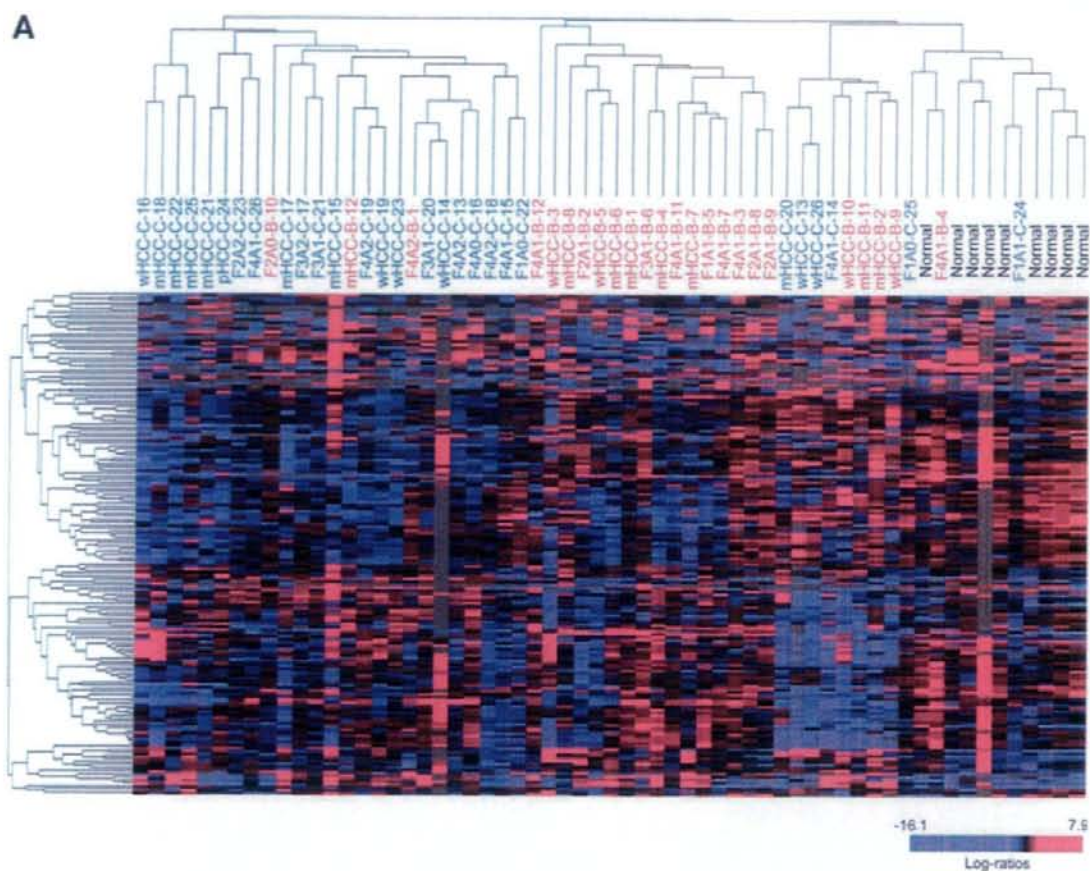
Fig. 2. (A) Hierarchical cluster analysis using total miRNA. Chronic hepatitis is indicated by histological stage and grade (F, fibrosis; A, activity) and type of infecting virus (B or C). HCC is indicated by histological grade (w, well differentiated; m, moderately differentiated; p, poorly differentiated) and type of infecting virus (B or C), with the patient number added at the end. (B) Relationship between five classes divided by binary tree classification. Expression profiles were first classified into normal liver and non-normal liver groups (node 1), then into HBV and HCV groups (node 2). The HBV group was further divided into HCC-B and CH-B (node 3), and the HCV group into HCC-C and CH-C (node 4).
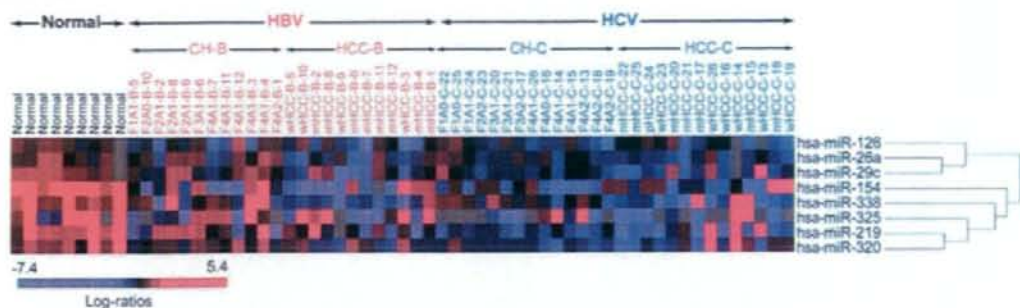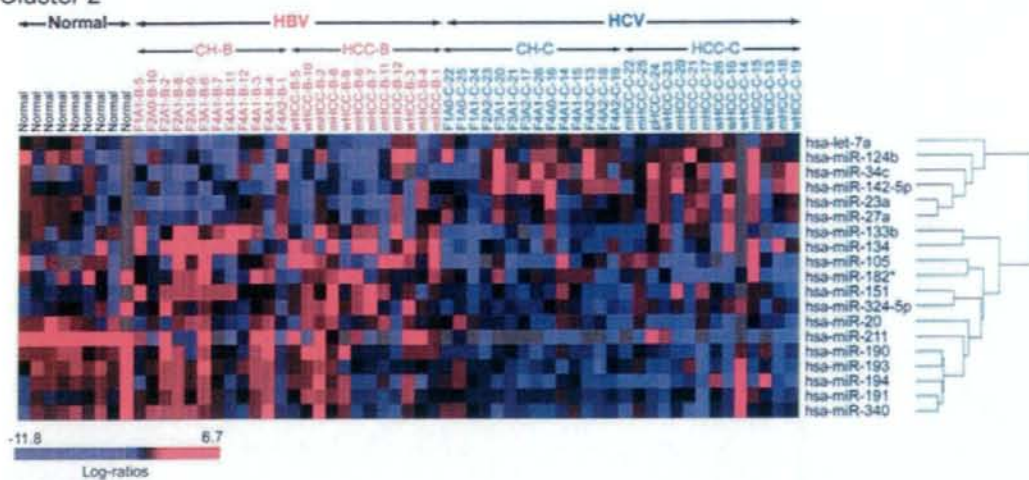
Fig. 3. Cluster 1: Eight miRNAs specifically differentiated node 1 classification. Cluster 2: Nineteen miRNAs specifically differentiated node 2 classification. Cluster 3: Twenty-three miRNAs differentiated CH-B and HCC-B as well as CH-C and HCC-C.

Fig. 4. Analysis of miRNA expression data. Target genes of miRNAs were predicted using MIRANDA Pro3.0; candidate target genes spotted on microarray were identified; number of genes that actually exhibit significant ($P < 0.05$) changes in expression among the genes was determined; and signal pathways involving genes regulated by the miRNAs that had exhibited differential expression between each group were analyzed using MetaCore (Table 4).

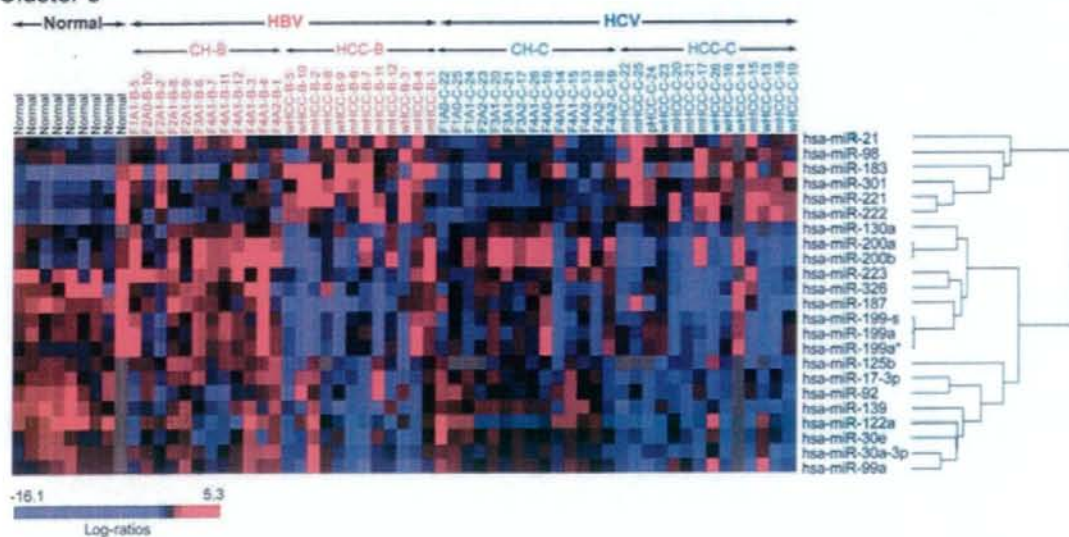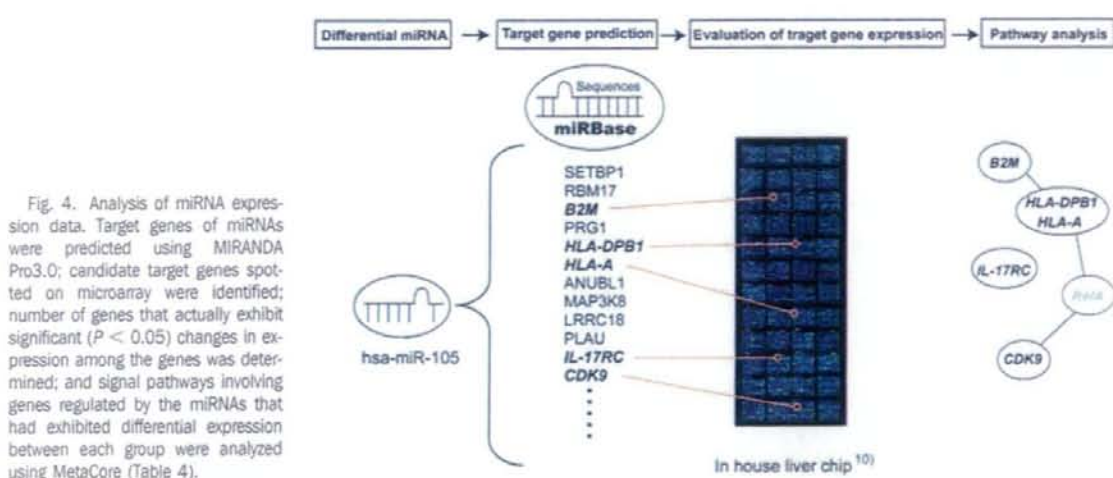roughly classified into normal liver, HBV-infected liver (CH-B+HCC-B; HBV group), and HCV-infected liver (CH-C+HCC-C; HCV group) (Fig. 2A). HCV viremia in two patients with CH-C was persistently cleared by interferon therapy before HCC development. The background liver of one of these patients was clustered in the normal group and those of others in the HCV group. Although these two patients were not clearly differentiated from others, some miRNAs such as miR-194, miR-211, and miR-340 that were down-regulated in the HCV group were significantly up-regulated in two patients (Fig. 3, cluster 2).

The present CH and HCC expression data were obtained from the same patient; however, each sample clustered irrespective of pairs in all but two patients. miRNA expression profiling was therefore more dependent on the disease condition than on the paired condition, as also confirmed by the Dunnett test.[12] We then attempted to classify the expression profiles into HBV and HCV groups using supervised learning methods (Table 2-1). HBV and HCV groups were significantly differentiated at an 87% accuracy ($P < 0.001$). The normal liver and CH (CH-B + CH-C)

and CH and HCC (HCC-B + HCC-C) were also significantly differentiated at a 90% rate of accuracy. These results suggest that different stages of liver disease (normal, CH, and HCC) can be differentiated from each other based on the miRNA expression profile, as well as HBV and HCV infection.

To examine the relationship among five categories of groups, namely, N, CH-B, CH-C, HCC-B and HCC-C, we attempted to differentiate the five groups using a supervised learning algorithm (binary tree classification) used for classifying three or more groups. SVM was used as a prediction method. Expression profiles were first classified into groups N (normal) and non-N (non-normal) (CH-C, CH-B, HCC-C, and HCC-B) (node 1) ($P < 0.01$). The non-N group was then classified into HBV and HCV (node 2) ($P < 0.01$). The HBV group was further classified into CH-B and HCC-B (node 3) ($P < 0.01$), and the HCV group was further classified into CH-C and HCC-C (node 4) ($P < 0.01$) (Fig. 2B, Table 2-2). Thus, the findings support the notion that differences in miRNA

Table 2-1. Class Prediction

No.	Class	Prediction (%)	No. of Predictors	P Value
1	HBV versus HCV	87	32	<0.001
2	N versus CH (B+C)	91	26	0.007
3	CH (B+C) versus HCC (B+C)	92	34	0.003

Class prediction algorithm was used for the classification of two groups of patients. Feature selection was based on the univariate significance level (alpha = 0.01). The support vector machine classifier was used for class prediction.
Abbreviations: CH, nontumor lesion of HCC; HCC, hepatocellular carcinoma; N, normal.

Table 2-2 Binary Tree Classification

Node	Group 1 Class	Group 2 Class	No. of Predictors	Misclassification Rate (%)
1	HCC-B, HCC-C, CH-B, CH-C	N	20	4.9
2	HCC-B, CH-B	HCC-C, CH-C	19	13.5
3	HCC-B	CH-B	15	29.2
4	HCC-C	CH-C	14	17.9

Binary tree classification algorithm was used for the classification of each category of patients. Feature selection was based on the univariate significance level (alpha = 0.01). The support vector machine classifier was used for class prediction. There were four nodes in the classfication tree.
Abbreviations: CH-B, non-tumor lesion of HCC-B; CH-C, nontumor lesion of HCC-C; HCC-B, hepatitis B virus-related hepatocellular carcinoma; HCC-C, hepatitis C virus-related hepatocellular carcinoma; N, normal

Table 3-1. Representative miRNAs That Were Commonly Repressed in CH-B, CH-C, HCC-B, and HCC-C Compared with Normal Liver (Cluster)

miRNA	Parametric P Value	Ratio*	No. of Significant Genes/Predicted Target Genes†	Hotelling Test P Value‡	Differentially Expressed Target Genes§	Pathway of Regulated Genes¶
hsa-miR-219	7.3E-05	0.28	25/109	2.59E-04	Glypican-3, ERP5, PLK2, HIRA, HMG2 ACOX1 NF-X1	Regulatory T cell differentiation Fatty acid beta-oxidation MHC class II biosynthetic process
hsa-miR-320	9.8E-05	0.50	26/88	3.50E-06	Vimentin, ALP (N-acetyltransferase-like), SEC61 beta, G-protein alpha-i2, Filamin A Rac1, RhoG Vinexin beta, Profilin I, Ca-ATPase3	Protein kinase cascade Organelle organization and biogenesis Actin cytoskeleton organization and biogenesis
hsa-miR-154	2.7E-04	0.15	22/70	5.40E-06	OTR, NET1(TSPAN1), NAP1, Vimentin, PDIA3, cytochrome P-450 reductase DLX2 GUAC, ACAT1	Regulation of apoptosis Morphogenesis Branched chain family amino acid catabolic process
hsa-miR-29c	1.8E-03	0.55	53/133	1.00E-06	FBXO7, ASPP1, HSPA4, Cathepsin O, PDF, COL4A1, HSPA4, TIP30, CXADR NS1-BP, ALP (N-acetyltransferase-like), ACTR10, Beclin 1 SMAD6, LTBR(TNFRSF3), ENPP7	Cell-substrate adhesion Transcription, DNA-dependent Apoptosis
hsa-miR-338	5.2E-03	0.46	30/101	3.60E-06	ID3, GATA-4, NFIA, FR-beta, CREST, HYOU1 G3ST1, CAD, FKBP12, LZIP, PDIA3, Schwannomin (NF2), CREST	Developmental process Immune effector process Immune system process
hsa-miR-26a	6.3E-03	0.70	37/119	2.64E-05	LIG4, c-FLIP, GADD45 beta, DAPK1, PRDX4, LRP130 Cyclin E, ZDHHC6, Tx1, ATG8 (GATE-16), WASP, C1s COPG1	Response to stimulus DNA replication initiation Ion transport
hsa-miR-126	8.1E-03	0.65	27/101	4.04E-03	ANP32B (apnl), HSPA4, RLI, LIV-1 (SLC39A6), PTP-MEG2, CD97, DHPR NFKBIA, NMI, MDH1, PDCD2 SMAD6, ATP6AP2, ANP32B (april), NMI, HSPA4	Regulation of cellular protein metabolic process Response to stress Apoptosis
hsa-miR-325	8.7E-03	0.20	18/63	2.03E-04	TRADD, CREST, NEDD8, annexin IV, GPX2, PDF, TNFAIP1 Glypican-3, ID1, PC-TP, SNRPB (Sm-B)	Developmental process Multicellular organismal development RNA splicing

*Ratio of HCC-B, HCC-C, CH-B, and CH-C to normal.

†The number of significant genes (P < 0.05) out of predicted target genes in which expression was evaluated in microarray.

‡Statistical assessment of presence of differentially expressed genes out of predicted target genes of miRNAs.

§Representative differentially expressed genes out of predicted target genes of miRNAs.

¶Representative pathway of differentially expressed genes out of predicted target genes of miRNAs.

expression between HBV and HCV are as distinct as those between CH and HCC.

Out of 20 miRNAs that differentiated node 1 classification (Table 2-2), 12 also differentiated node 3 or node 4 classification. The remaining eight miRNAs specifically differentiated node 1 classification. They were down-regulated in the HBV and HCV groups compared with the normal group (Fig. 3, cluster 1). Nineteen miRNAs differentiated node 2 classification (Table 2-2) and the hierarchical clustering using these miRNAs clearly differentiated the HBV and

HCV groups (Fig. 3, cluster 2). There were 15 and 14 miRNAs that differentiated node 3 and 4 classifications, respectively (Table 2-2). Hierarchical clustering using these miRNAs revealed that these miRNAs differentiated CH-B and HCC-B as well as CH-C and HCC-C, respectively; 17 miRNAs were down-regulated in HCC, and six were up-regulated in HCC (Fig. 3, cluster 3).

These results indicate that there were two types of miRNAs—one associated with HBV and HCV infection (cluster 2), the other associated with the stages of liver

Table 4-1. Pathway Analysis of Targeted Genes by miRNAs that Were Commonly Repressed in CH-B, CH-C, HCC-B, and HCC-C Compared with Normal Liver (Cluster 1)

No.	Pathway Name	P Value
	Down-regulated miRNA in CH-B,HCC-B,CH-C and HCC-C (possibly up-regulating target genes)	
1	Cell adhesion_Platelet-endothelium-leukocyte interactions	1.11E-02
2	Cell cycle_S phase	2.18E-02
3	Protein folding_Protein folding nucleus	2.43E-02
4	Cell cycle_G1-S	3.07E-02
5	Development_Cartilage development	3.89E-02
6	Protein folding_Folding in normal condition	3.89E-02
7	Proteolysis_Connective tissue degradation	3.99E-02
8	Proteolysis_Proteolysis in cell cycle and apoptosis	4.31E-02
9	Signal Transduction_BMP and GDF signaling	5.81E-02
10	Immune_Antigen presentation	6.05E-02

disease (clusters 1 and 2) that were irrelevant to the differences in HBV and HCV infection.

Differential miRNAs and Their Candidate Target Genes and Signaling Pathways. Differentially expressed miRNAs are shown in Table 3. In addition to the expression ratios of miRNAs in each group, the number of genes analyzed on the microarray predicted to be the target genes of miRNAs and that which actually showed significant ($P < 0.05$) differences in expression are also shown. Based on the frequencies and levels of expression of differential genes, the significance of regulation of these gene groups by miRNAs was evaluated using Hotelling T2 test (BRB ArrayTools) (Table 3). The representative candidate target genes and their signaling pathways by each miRNA were shown one by one (Table 3). The signaling pathways regulated by all differential miRNAs in each category of groups are shown in Table 4.

Eight miRNAs were down-regulated in the HBV and HCV groups compared with the normal group (Table 3-1; Fig. 3, cluster 1). These miRNAs were associated with an increased expression of genes related to cell adhesion, cell cycle, protein folding, and apoptosis (Tables 3-1, 4-1), and possibly with the common feature of CH irrespective of the differences in HBV and HCV infection.

Nineteen miRNAs clearly differentiated the HBV and HCV groups (Fig. 3, cluster 2, Table 3-2). Thirteen miRNAs exhibited a decreased expression in the HCV group, and six showed a decreased expression in the HBV group. miRNAs exhibiting a decreased expression in the HCV group regulate genes related to immune response, antigen presentation, cell cycle, proteasome, and lipid metabolism. On the other hand, those exhibiting a decreased expression in the HBV group regulate genes related to cell death, DNA damage and recombination, and transcription signals. These findings reflected the differ-

ences in the gene expression profile between CH-B and CH-C described (Tables 3-2, 4-2).[10] Interestingly, although these miRNAs were HBV and HCV infection–specific, some of them were reported to be tumor-associated miRNAs, suggesting the possible involvement of infection-associated miRNAs in HCC development.

Twenty-three miRNAs clearly differentiated CH and HCC that were irrelevant to the differences in HBV and HCV infection. Seventeen miRNAs were down-regulated in HCC that up-regulated cancer-associated pathways such as cell cycle, adhesion, proteolysis, transcription, translation, and the Wnt signaling pathway (Tables 3-3, 4-3). Six miRNAs were up-regulated in HCC that down-regulated all inflammation-mediated signaling pathways, potentially reflecting impaired antitumor immune response.

Relationship Between Expressions of Infection-Associated miRNA in Liver and Cultured Cells Infected with HBV and HCV. To clarify whether the expression of infection-associated miRNA is regulated by HBV and HCV infection, we investigated the relationship between changes in miRNA in liver tissues and those in miRNA in Huh7.5 cells in which infectious HBV or HCV clones replicated. To evaluate the replication of each clones in Huh7.5 cells, we measured time-course changes in the amounts of HBV-DNA and HCV-RNA in Huh7.5 cells transfected with pHBV1.2 and JFH1-RNA, respectively, by RTD-PCR (Supplementary Fig. 1A). The expression of HBV proteins was examined by measuring the amount of HBeAg released in culture medium (Supplementary Fig. 1B). HCV protein expression was examined by evaluating the core protein expression after 48 hours by fluorescence immunostaining (Supplementary Fig. 1C). RNA was extracted from the Huh7.5 cells 48 hours after gene transfection, and miRNA expression pattern in the cells was compared with those in liver tissues. We found a strong correlation between differences in miRNA expression between liver tissues of the HBV and HCV groups, and those in miRNA expression between Huh7.5 cells transfected with HBV and HCV clones ($r = 0.73$, $P = 0.0006$) (Fig. 5). These results revealed that differences in the expression of infection-associated miRNA in the liver between the HBV and HCV groups are explained by changes in miRNA expression caused by HBV and HCV infections.

Verification of Regulation of Candidate Target Genes by miRNA. Small interfering RNAs (Ambion) specific to 13 miRNAs (has-miR-17*, has-miR-20a, has-miR-23a, has-miR-26a, has-miR-27a, has-miR-29c, has-miR-30a, has-miR-92, has-miR-126, has-miR-139, has-miR-187, has-miR-200a, and has-miR-223) showing significant differences in expression were transfected into

Table 3-2. Differentially Expessed miRNA Between HCC-B, CH-B, and HCC-C, CH-C, and Their Representative Target Genes (Cluster 2)

miRNA	Parametric P Value	Ratio*	No. of Significant Genes/Predicted Target Genes†	Hotelling Test P Value‡	Differentially Expressed Target Genes§	Pathway of Regulated Genes¶
hsa-miR-190	1.2E-05	2.06	21/68	4.47E-02	Chk1, C2orf25, VRK2, USP16, STAF65(gamma)	Regulation of cell cycle
					AP1S2, RNASE4	Mitotic cell cycle
					PPP2R1B, ARHGAP15, UBPY	Negative regulation of apoptosis
hsa-miR-134	2.3E-04	5.74	11/58	3.40E-06	VKDGC, SH2B, MALS-1, DDB2	Multicellular organismal process
					BCRP1	Regulation of viral reproduction
					DDB2	Lipid biosynthetic process
hsa-miR-151	2.8E-04	1.82	12/62	6.41E-01	RGS2, UFO, AK2, USP7	G-protein signaling
					eIF4G2, USP7	Regulation of translation
					SLC22A7	Organic anion transport
hsa-miR-193	5.0E-04	1.67	23/95	9.30E-01	G-protein alpha-11, p130CAS, VAV-1, PDCD11	Cell motility
					Colipase, ACSA	Energy coupled proton transport
					DCOR	Intracellular signaling cascade
hsa-miR-133b	1.7E-03	2.42	20/97	3.69E-02	DDB2, Bcl-3, Cystatin B	Proteasomal protein catabolic process
					Rab-3, RAG1AP1, KCNH2, DCOR	Regulation of biological quality
					AL1B1	Carbohydrate metabolic process
hsa-miR-324-5p	2.9E-03	1.51	27/121	1.90E-06	SKAP55, VAV-1, DDB2, E2A, NIP1	Cellular developmental process
					MEMO (CGI-27), Rab-3	Cellular structure morphogenesis
					COPG1, GPX3, OAZ2	Glutathione metabolic process
hsa-miR-182*	3.1E-03	2.23	28/123	< 1e-07	Alpha-endosulfine, HCCR-2, Thioredoxin-like 2, TPT1, USP7	Translation initiation in response to stress
					DDB2, TPT1	Cellular developmental process
					JIP-1	JNK cascade
hsa-miR-105	4.6E-03	4.38	18/68	4.74E-05	Beta-2-microglobulin, HLA-B27	Antigen processing and presentation
					PIMT, IL-17RC	Immune response
					MHC class I, CDK9, ERG1, Desmocollin 3	
hsa-miR-211	5.3E-03	25.61	10/56	2.00E-04	PSMD5, SLC26A6	Proteasomal protein catabolic process
hsa-miR-20	5.7E-03	1.52	27/113	5.28E-03	Noelin, SC4MOL, Thioredoxin-like 2, CCL5, NALP3	Regulation of apoptosis
					Hic-5/ARA55, USP16, MAP4, Ferroportin 1	Positive regulation of cellular process
					TOP3A, PLRP1	Oxygen transport
hsa-miR-191	6.7E-03	1.39	25/79	7.55E-04	CDK9, GPS2, CLTA, LXR-alpha	Nucleic acid metabolic process
					ACSA	Acetyl-CoA biosynthetic process
					UGCGL1, SGPP1	Metal ion transport
hsa-miR-340	8.5E-03	1.48	17/81	3.73E-03	FKBP12, DCOR,	Calcium ion transport
					Gelsolin, VAV-1, ARF6	Actin cytoskeleton organization and biogenesis
					HXK3	Glucose catabolic process
hsa-miR-194	8.7E-03	1.67	13/74	5.90E-01	Cyclin B1, Serglycin	M phase of mitotic cell cycle
					PTE2	Acyl-CoA metabolic process
					SLC7A6	Carbohydrate utilization
hsa-miR-23a	1.9E-04	0.46	14/97	< 1e-07	RGL2, MANR, MEK1 (MAP2K1), Caspase-3, AZGP1	Protein kinase cascade
					FRK, Pyk2(FAK2), CSE1L	Cellular developmental process
					AZGP1	Defense response
hsa-miR-142-5p	4.9E-04	0.40	25/89	9.10E-06	Sirtuin4, PAI2, PSAT, RIL, CDC34, SPRY1	Metabotropic glutamate receptor
					E4BP4, DNAJC12, WWP1, PAIP1, PASK, rBAT	Regulation of gene expression
					VCAM1, CaMK I, WWP1, FHL3	Cell-matrix adhesion
hsa-miR-34c	5.1E-04	0.20	31/129	7.30E-06	Diacylglycerol kinase, zeta, PLC-delta 1, ATP2C1, PAI2	Manganese ion transport
					MLK3(MAP3K11), MEK1(MAP2K1), CDC25C, MRF-1, XPC	Protein kinase cascade
					GNT-IV	Inflammatory cell apoptosis

miRNA	Parametric P Value	Ratio*	No. of Significant Genes/Predicted Target Genes†	Hotelling Test P Value‡	Differentially Expressed Target Genes§	Pathway of Regulated Genes¶
hsa-miR-124b	8.6E-04	0.32	25/120	7.10E-05	E2F5, Rad51, Jagged1 MLK3(MAP3K11), RGS1 COL16A1	Muscle development Intracellular signaling cascade MAPKKK cascade
hsa-let-7a	1.0E-03	0.45	28/136	9.35E-04	RAD51C, CoAA, hASH1, Cockayne syndrome B, Caspase-1, PP5 PLC-delta 1, MANR, ACADVL HGF, NGF	Response to DNA damage stimulus Fibroblast proliferation Cellular developmental process
hsa-miR-27a	3.9E-03	0.59	18/108	1.19E-02	COL16A1, RIL, RhoGDI gamma, ANP32B (april) VE-cadherin, NTH1, GATA-2, E4BP4 RAD51C	Cytoskeleton organization and biogenesis Response to external stimulus DNA recombination

*Ratio of HCC-B, CH-B, to HCC-C,CH-C.
†The number of significant genes (p <0.05) out of predicted target genes in which expression was evaluated in microarray.
‡Statistical assesment of presence of differentially expressed genes out of predicted target genes of miRNAs.
§Representative differentially expressed genes out of predicted target genes of miRNAs.
¶Representative pathway of differentially expressed genes out of predicted target genes of miRNAs.

Huh7 cells to examine loss of function of the miRNAs. Five miRNAs (has-miR-23a, has-miR-26a, has-miR-27a, has-miR-92, and has-miR-200a) showed a decreased expression by more than 50%. Precursor miRNAs of these miRNAs were also transfected into the cells to examine the gain of function of the miRNAs (Supplementary Fig. 2). It was confirmed that the expressions of target genes of the five miRNAs (LIG4 [by has-miR-26a]; RGL2 [by

has-miR-23a]; Rad51C [by has-miR-27a]; KAP3, CDC25B, KAP3, CDK2AP2, POLD, and CPSF4 [by has-miR-200a]; and TUBGCP2, SNX15 and BCAT2 [by has-miR-92]) were increased by the suppression of the miRNAs induced by small interfering RNAs and were decreased by the overexpression of precursor miRNAs (Supplementary Fig. 3).

Discussion

miRNA plays an important role in various diseases such as infection and cancer.[1-3] In this study, we examined miRNA expression profiles in normal liver and HCC, including nontumor lesions infected with HBV or HCV. Although the expression profiles of miRNAs in HCC have been reported,[16-18] most of the studies were performed using a microarray system. Because we thought that miRNAs could not produce enough detection signals owing to their short length, we applied a highly sensitive and quantitative RTD-PCR method for miRNAs. Moreover, global gene expression in the same tissues was analyzed via cDNA microarray to examine whether the differentially expressed miRNAs could regulate their target genes. Because the absolute standard of miRNA is not available at present, and miRNA expression was compared within the samples and genes analyzed in this study, there might be possible errors when a larger number of samples and genes were analyzed.

Using these systems, we found that the expression profile in miRNAs was clearly different according to HBV and HCV infection for the first time. The differences were confirmed by the nonsupervised learning method, hierarchical clustering (Fig. 2A), and supervised learning methods based on SVM at an 87% accuracy ($P < 0.001$)

Table 4-2. Pathway Analysis of Targeted Genes by Differentially Expressed miRNAs Between HBV-Related Liver Disease (CH-B,HCC-B) and HCV Related Liver Disease (CH-C,HCC-C Cluster 2)

No.	Pathway Name	P Value
Down-regulated miRNA in CH-C,HCC-C (possibly up-regulating target genes)		
1	Immune_Phagosome in antigen presentation	5.80E-04
2	Muscle contraction	1.05E-03
3	Immune_Antigen presentation	5.75E-03
4	Cell cycle_Meiosis	1.49E-02
5	Reproduction_Male sex differentiation	2.06E-02
6	Cell adhesion_Platelet aggregation	2.77E-02
7	Transport_Synaptic vesicle exocytosis	3.56E-02
8	Inflammation_Kallikrein-kinin system	3.73E-02
9	Inflammation_IgE signaling	4.10E-02
10	Development_Skeletal muscle development	5.02E-02
Down-regulated miRNA in CH-B,HCC-B (possibly up-regulating target genes)		
1	Signal Transduction_Cholecystokinin signaling	1.15E-04
2	Inflammation_NK cell cytotoxicity	5.29E-03
3	Signal transduction_CREM pathway	5.31E-03
4	Reproduction_GnRH signaling pathway	7.80E-03
5	DNA damage_DBS repair	1.02E-02
6	Cell cycle_G2-M	1.63E-02
7	Development_Neuromuscular junction	2.07E-02
8	Apoptosis_Apoptosis mediated by external signals	2.42E-02
9	Reproduction_FSH-beta signaling pathway	2.92E-02
10	Cell adhesion_Amyloid proteins	3.81E-02

Table 3-3. Differentially Expessed miRNA Between CH and HCC and Their Representative Target Genes (Cluster 3)

miRNA	Parametric p-value	Ratio*	No. of Significant Genes/Predicted Target Genes†	Hotelling Test P Value‡	Differentially Expressed Target Genes§	Pathway of Regulated Genes¶
hsa-miR-139	4.50E-06	0.42	19/106	2.70E-03	Cyclin B1, DHX15, MCM5, Histone H2A RBCK1, SYHH	Mitotic cell cycle Protein catabolic process
					ILK, IGFBP7, SAFB, CTR9	Response to external stimulus
hsa-miR-30a-3p	2.50E-05	0.49	26/144	1.73E-02	GGH, Pirin, ZNF207, Annexin VII	Regulation of oxidoreductase activity
					ILK, LTA4H, ABC50, GNPAT	Cell-matrix adhesion
					DLC1	Morphogenesis
hsa-miR-130a	7.00E-05	0.50	22/108	1.07E-02	SPHM, PPP2R5D, RHEB2, SPHM	Mitotic cell cycle
					MLK3(MAP3K11), Otubain1, TIMP4	Protein modification process
					NRBP	Cell differentiation
hsa-miR-223	3.40E-04	0.39	14/90	6.52E-03	Ephrin-A1, Midkine, FDPS	Cell morphogenesis
					K(+) channel, subfamily J	Notch signaling pathway
hsa-miR-187	3.55E-04	0.12	16/66	6.76E-04	HFE2, Otubain1	Negative regulation of programmed cell death
					PRSS11, SUPT5H, RAG1AP1	Developmental process
					PLOD3	Mitochondrial ornithine transport
hsa-miR-200a	6.86E-04	0.18	20/141	2.15E-02	CDC25B, KAP3, CDK2AP2, CHKA	Cell communication
					POLD	DNA replication
					CPSF4	RNA splicing
hsa-miR-17-3p	8.42E-04	0.58	28/108	8.98E-04	MLK3(MAP3K11), Tip60, ACBD6, DOC-1R, DAX1, RBCK1	Protein kinase cascade
					WNT5A, 14-3-3 gamma, DHX15	BMP signaling pathway
					HFE2, MCM5	DNA recombination
hsa-miR-99a	1.17E-03	0.53	33/163	9.52E-03	Calpain small subunit, Thoredoxin-like 2, Survivin	Cytokinesis
					IBP2, DNA-PK, KAP3,	Intracellular signaling cascade
					NFE2L1, PARP-1, HDAC11	Regulatory T cell differentiation
hsa-miR-200b	1.57E-03	0.18	24/147	2.72E-02	HSP47, HMG2, NRBP	Regulation of cell cycle
					SNX17	Cell motility
					Ephrin-A1	Receptor protein signaling pathway
hsa-miR-125b	1.82E-03	0.55	26/114	1.03E-01	COL4A2, TIP30, HSP47, MSP58	Cell adhesion
					MLK3(MAP3K11), ERK2 (MAPK1), ERK1 (MAPK3), PLOD3	Nuclear translocation of MAPK
					Otubain1, SCN4A(SkM1)	Ubiquitin-dependent protein catabolic process
hsa-miR-30e	2.10E-03	0.65	24/151	4.30E-02	Cyclin B1, XTP3B, GAK, Annexin VII, MIC2, NRBP	Mitotic cell cycle
					MSS4	Protein localization
					S100A10	Calcium ion transport
hsa-miR-199a*	4.26E-03	0.35	11/71	7.16E-02	BUB3, Cyclin B1, LMNBR	Mitotic cell cycle
					PRAME	Cardiac muscle cell differentiation
hsa-miR-122a	6.31E-03	0.51	11/80	1.01E-03	JAB1, APEX, Clathrin heavy chain	Base-excision repair
					PARN	Translational initiation
					DDAH2	Regulation of cellular respiration
hsa-miR-199a	8.77E-03	0.35	18/94	3.56E-02	IL-13, MLK3(MAP3K11), CLK2, ACP33	Protein amino acid phosphorylation
					PAFAH beta, SPA1, CLCN4	Small GTPase mediated signal transduction
hsa-miR-326	9.00E-03	0.57	29/147	2.25E-01	Midkine, ENT1, IP3KA, PSMC5, ANCO-1	Regulation of programmed cell death
					Thy-1, MCM6, Tip60, VILIP3	Cell-matrix adhesion
					COMP, Cathepsin A	Blood vessel development
hsa-miR-92	9.60E-03	0.81	28/140	2.47E-02	TUBGCP2, Fibrillin 1, PIPKI gamma, KAP3	Rho protein signal transduction
					SNX15, BCAT2	LDL receptor and BCAA metabolism
					IGFBP7, FZD6, COPS6	Adenosine receptor signaling pathway
hsa-miR-221	3.40E-06	3.34	16/67	3.59E-01	Lck, Kallistatin, Neuromodulin, LFA-3, PA24A, AZGP1, MSH2	Immune response-activating signal transduction
					KYNU, PMCA3	DNA repair

Table 3-3. *Continued*

miRNA	Parametric p-value	Ratio*	No. of Significant Genes/Predicted Target Genes†	Hotelling Test P Value‡	Differentially Expressed Target Genes§	Pathway of Regulated Genes¶
hsa-miR-222	6.50E-06	2.23	18/85	1.59E-02	Thrombospondin 1, Lck, MSH2, ATF-2, CITED2, Kallistatin	Cell motility
					PGAR	Triacylglycerol metabolic process
					KYNU	DNA replication
hsa-miR-301	5.22E-05	1.96	14/71	1.16E-01	Beta-2-microglobulin, PPCKM, PRC, Fra-1, PPCKM, ACAT2	Antigen processing and presentation
					BMPR1B, ARMER, EHM2, RBBP8	Meiotic recombination
					Neuromodulin, LDLR	Cell motility
hsa-miR-21	7.67E-03	1.57	19/81	1.86E-04	Btk, Fra-1, MSH2, Collectrin, Adipophilin	Regulation of T cell proliferation
					RNASE4, AGXT2L1	Peptidyl-tyrosine phosphorylation
					SARDH	Natural killer cell activation during immune response
hsa-miR-183	2.46E-02	3.51	13/86	3.36E-01	Hdj-2, PEMT, Lck, MKP-5, Chondromodulin-I, ABCA8	Cell differentiation
					IL-16, MTRR, SerRS	Methionine biosynthetic process
hsa-miR-98	5.22E-02	1.32	24/130	2.95E-04	ACAA2, LTB4DH, ACADVL, DECR, S14 protein,	Fatty acid metabolic process
					Rapsyn, Kallistatin, ENPEP, Beta crystallin B1	Multicellular organismal process
					CYP4F8	Prostaglandin metabolic process

*Ratio of HCC to CH.

†The number of significant genes ($P<0.05$) out of predicted target genes in which expression was evaluated in microarray.

‡Statistical assesment of presence of differentially expressed genes out of predicted target genes of miRNAs.

§Representative differentially expressed genes out of predicted target genes of miRNAs.

¶Representative pathway of differentially expressed genes out of predicted target genes of miRNAs.

Table 4-3. The Pathway Analysis of Targeted Genes by Differentially Expressed miRNAs Between CH and HCC (Cluster 3)

No.	Pathway Name	P Value
	Down-regulated miRNA in HCC (possibly up-regulating target genes)	
1	Cytoskeleton_Spindle microtubules	2.15E-03
2	Transcription_Chromatin modification	5.27E-03
3	Proteolysis_Ubiquitin-proteasomal proteolysis	6.43E-03
4	Cell adhesion_Cell-matrix interactions	7.30E-03
5	Cell cycle_Meiosis	7.83E-03
6	DNA damage_Checkpoint	1.69E-02
7	Reproduction_Progesterone signaling	1.94E-02
8	Apoptosis_Apoptotic mitochondria	3.14E-02
9	Translation_Regulation of initiation	4.22E-02
10	Signal transduction_WNT signaling	4.26E-02
	Up-regulated miRNA in HCC (possibly down-regulating target genes)	
1	Inflammation_IgE signaling	1.05E-02
2	Inflammation_Kallikrein-kinin system	2.46E-02
3	Inflammation_Innate inflammatory response	2.51E-02
4	Inflammation_Histamine signaling	4.25E-02
5	Inflammation_Neutrophil activation	4.55E-02
6	Chemotaxis	4.68E-02
7	Inflammation_IL-12,15,18 signaling	5.16E-02
8	Inflammation_NK cell cytotoxicity	7.25E-02
9	Cell cycle_G0-G1	7.53E-02
10	Inflammation_Complement system	7.72E-02

(Table 2-1). As similarly described, the expression profile in miRNAs was significantly different according to the progression of liver disease (normal, CH, and HCC) in this study. The present CH and HCC expression data were derived from the same patient, and some microarray analyses suggested that the noncancerous liver tissue can predict the prognosis of HCC.[19,20] We examined whether the miRNA expression of paired samples was similar or independent using the Dunnett test[12] (Supplementary Data). Our data indicated that miRNA expression profiling was more dependent on the disease condition than on the paired condition, although the issue of paired samples should be taken into account carefully.

Binary tree prediction analysis and detailed assessment of hierarchical clustering revealed two types of differential miRNAs, one associated with HBV and HCV infection, the other associated with the stages of liver disease that were irrelevant to the differences in HBV and HCV infection. We found that differences in miRNA expression between liver tissues with HBV and HCV (HBV/HCV) were strongly correlated with those in miRNA between cultured cell models of HBV and HCV infection (HBV/HCV) ($r = 0.73$ $P = 0.0006$) (Fig. 5). Thus, there exist HBV- and HCV-infection–specific miRNAs that potentially regulate viral replication and host gene signaling pathways in hepatocytes.
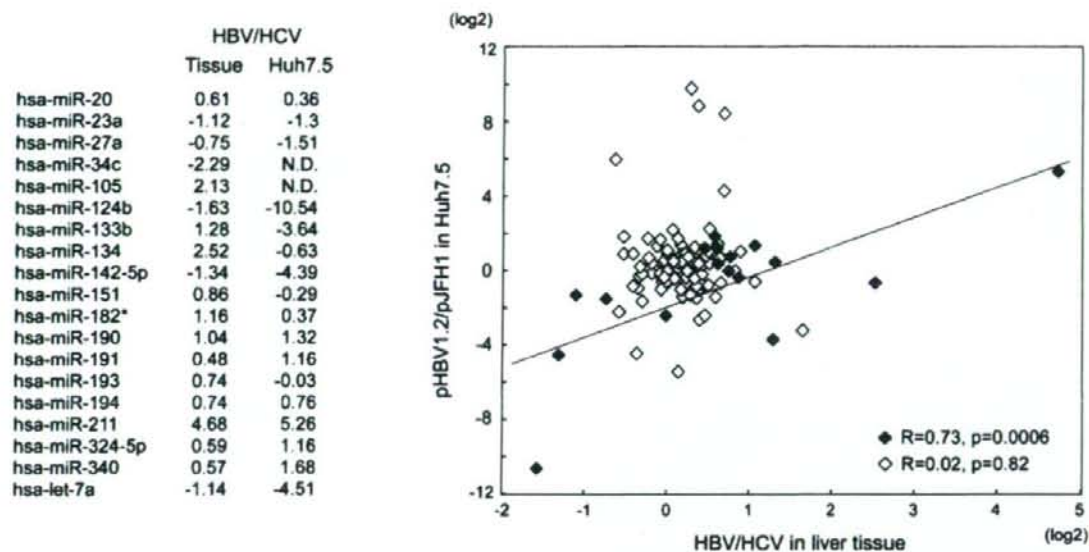
	HBV/HCV	
	Tissue	Huh7.5
hsa-miR-20	0.61	0.36
hsa-miR-23a	-1.12	-1.3
hsa-miR-27a	-0.75	-1.51
hsa-miR-34c	-2.29	N.D.
hsa-miR-105	2.13	N.D.
hsa-miR-124b	-1.63	-10.54
hsa-miR-133b	1.28	-3.64
hsa-miR-134	2.52	-0.63
hsa-miR-142-5p	-1.34	-4.39
hsa-miR-151	0.86	-0.29
hsa-miR-182*	1.16	0.37
hsa-miR-190	1.04	1.32
hsa-miR-191	0.48	1.16
hsa-miR-193	0.74	-0.03
hsa-miR-194	0.74	0.76
hsa-miR-211	4.68	5.26
hsa-miR-324-5p	0.59	1.16
hsa-miR-340	0.57	1.68
hsa-let-7a	-1.14	-4.51

Fig. 5. Correlation between differences in miRNA expression between liver tissues infected with HBV and HCV and those in miRNA expression between cultured cell models of HBV and HCV infections. A total of 140 of 188 miRNAs were confirmed to be expressed in Huh7.5 cells. There was a significant correlation of infection-associated miRNA (closed lozenge) in vitro and in vivo ($r = 0.73$, $P = 0.0006$), but none for the other 121 miRNAs (open lozenge) ($r = 0.02$, $P = 0.82$).

The pathway analysis of targeted genes by miRNAs revealed that 13 miRNAs exhibiting a decreased expression in the HCV group regulate genes related to immune response, antigen presentation, cell cycle, proteasome, and lipid metabolism. Six miRNAs showing a decreased expression in the HBV group regulate genes related to cell death, DNA damage and recombination, and transcription signals. These findings reflected differences in the gene expression profile between CH-B and CH-C as described.[10] Many of the miRNAs were down-regulated in the HCV group rather than in the HBV group. It has been reported that human endogenous miRNAs may be involved in defense mechanisms, mainly against RNA viruses.[21] On the other hand, it is suggested that endogenous miRNAs may be consumed and reduced by defense mechanisms, especially those against RNA viruses.

Although the expressions of these HBV- and HCV-infection–specific miRNAs were irrelevant to the differences in CH and HCC (Fig. 3, cluster 2), some of them have been reported to play pivotal roles in the occurrence of cancer. For example, has-let-7a regulates ras and c-myc genes,[22] and has-miR-34 is involved in the p53 tumor suppressor pathway.[23] These miRNAs were down-regulated in the HBV group, possibly participating in a more aggressive and malignant phenotype in HCC-B rather than in HCC-C. High expression of has-miR-191 was shown to be significantly associated with the worse survival in acute myeloid leukemia,[24] and has-miR-191 was

overexpressed in the HBV group compared with the HCV group. On the other hand, has-miR-133b, which was reported to be down-regulated in squamous cell carcinoma,[25] was repressed in the HCV group compared with the HBV group. Some hematopoietic-specific miRNAs such as has-miR-142-5p were up-regulated in the HCV group. Therefore, these miRNAs were not only HBV and HCV infection–associated but also tumor-associated. These findings indicate different mechanisms of development of HCC infected with HBV and HCV (Fig. 6).

Following HCC development, common changes in miRNA expression between HCC-B and HCC-C appeared (Fig. 3, cluster 3). The 23 miRNAs mentioned above clearly differentiated CH and HCC that were irrelevant to the differences in HBV and HCV infections. Seventeen miRNAs were down-regulated in HCC, which up-regulated cancer-associated pathways. Six miRNAs were up-regulated in HCC that down-regulated all inflammation-mediated signaling pathways, potentially reflecting impaired antitumor immune response in HCC. These results suggest that common signaling pathways are involved in HCC development from CH, and that HBV- and HCV-specific miRNAs participate in generating HCC-specific miRNA expressions (Fig. 6). Therefore, these miRNAs might be good candidates for molecular targeting to prevent HCC occurrence, because they reg-
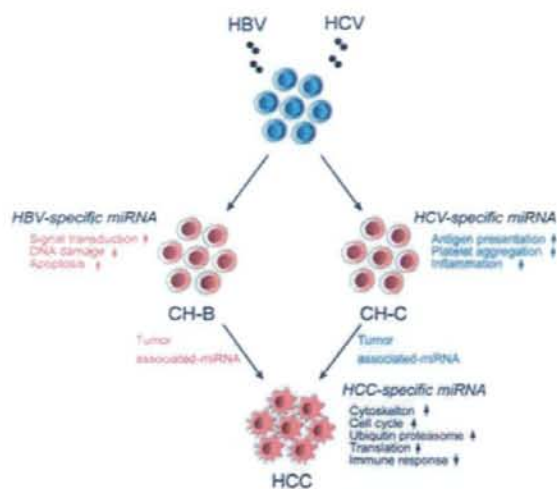
Fig. 6. Infection-associated and HCC-specific miRNAs and liver disease progression.

ulate a common signaling pathway underlying HCC-B and HCC-C development.

In conclusion, we showed that miRNAs are important mediators of HBV and HCV infections as well as liver disease progression. Further studies are needed to enable more detailed mechanistic analysis of the miRNAs identified here and to evaluate the usefulness of miRNAs as diagnostic/prognostic markers and potential therapeutic target molecules.

References

1. He L, Thomson JM, Hemann MT, Hernando-Monge E, Mu D, Goodson S, et al. A microRNA polycistron as a potential human oncogene. Nature 2005;435:828-833.

2. Calin GA, Dumitru CD, Shimizu M, Bichi R, Zupo S, Noch E, et al. Frequent deletions and down-regulation of micro-RNA genes miR15 and miR16 at 13q14 in chronic lymphocytic leukemia. Proc Natl Acad Sci U S A 2002;99:15524-15529.

3. Cho WC. OncomiRs: the discovery and progress of microRNAs in cancers. Mol Cancer 2007;6:60.

4. Hutvagner G, Zamore PD. A microRNA in a multiple-turnover RNAi enzyme complex. Science 2002;297:2056-2060.

5. Ambros V, Bartel B, Bartel DP, Burge CB, Carrington JC, Chen X, et al. A uniform system for microRNA annotation. RNA 2003;9:277-279.

6. Lee RC, Feinbaum RL, Ambros V. The C. elegans heterochronic gene lin-4 encodes small RNAs with antisense complementarity to lin-14. Cell 1993;75:843-854.

7. Lewis BP, Burge CB, Bartel DP. Conserved seed pairing, often flanked by adenosines, indicates that thousands of human genes are microRNA targets. Cell 2005;120:15-20.

8. Kiyosawa K, Sodeyama T, Tanaka E, Gibo Y, Yoshizawa K, Nakano Y, et al. Interrelationship of blood transfusion, non-A, non-B hepatitis and hepatocellular carcinoma: analysis by detection of antibody to hepatitis C virus. HEPATOLOGY 1990;12:671-675.

9. Honda M, Kaneko S, Kawai H, Shirota Y, Kobayashi K. Differential gene expression between chronic hepatitis B and C hepatic lesion. Gastroenterology 2001;120:955-966.

10. Honda M, Yamashita T, Ueda T, Takatori H, Nishino R, Kaneko S. Different signaling pathways in the livers of patients with chronic hepatitis B or chronic hepatitis C. HEPATOLOGY 2006;44:1122-1138.

11. Molinaro AM, Simon R, Pfeiffer RM. Prediction error estimation: a comparison of resampling methods. Bioinformatics 2005;21:3301-3307.

12. Dunnett CW. A multiple comparison procedure for comparing several treatments with a control. J Am Stat Assoc 1955;50:1096-1121.

13. Weiss L, Kekule AS, Jakubowski U, Burgelt E, Hofschneider PH. The HBV-producing cell line HepG2-4A5: a new in vitro system for studying the regulation of HBV replication and for screening anti-hepatitis B virus drugs. Virology 1996;216:214-218.

14. Lindenbach BD, Evans MJ, Syder AJ, Wolk B, Tellinghuisen TL, Liu CC, et al. Complete replication of hepatitis C virus in cell culture. Science 2005;309:623-626.

15. Wakita T, Pietschmann T, Kato T, Date T, Miyamoto M, Zhao Z, et al. Production of infectious hepatitis C virus in tissue culture from a cloned viral genome. Nat Med 2005;11:791-796.

16. Murakami Y, Yasuda T, Saigo K, Urashima T, Toyoda H, Okanoue T, et al. Comprehensive analysis of microRNA expression patterns in hepatocellular carcinoma and non-tumorous tissues. Oncogene 2006;25:2537-2545.

17. Varnholt H, Drebber U, Schulze F, Wedemeyer I, Schirmacher P, Dienes HP, et al. MicroRNA gene expression profile of hepatitis C virus-associated hepatocellular carcinoma. HEPATOLOGY 2008;47:1223-1232.

18. Budhu A, Jia HL, Forgues M, Liu CG, Goldstein D, Lam A, et al. Identification of metastasis-related microRNAs in hepatocellular carcinoma. HEPATOLOGY 2008;47:897-907.

19. Budhu A, Forgues M, Ye QH, Jia HL, He P, Zanetti KA, et al. Prediction of venous metastases, recurrence, and prognosis in hepatocellular carcinoma based on a unique immune response signature of the liver microenvironment. Cancer Cell 2006;10:99-111.

20. Hoshida Y, Villanueva A, Kobayashi M, Peix J, Chiang DY, Camargo A, et al. Gene expression in fixed tissues and outcome in hepatocellular carcinoma. N Engl J Med 2008;359:1995-2004.

21. Jopling CL, Yi M, Lancaster AM, Lemon SM, Sarnow P. Modulation of hepatitis C virus RNA abundance by a liver-specific MicroRNA. Science 2005;309:1577-1581.

22. Johnson CD, Esquela-Kerscher A, Stefani G, Byrom M, Kelnar K, Ovcharenko D, et al. The let-7 microRNA represses cell proliferation pathways in human cells. Cancer Res 2007;67:7713-7722.

23. He X, He L, Hannon GJ. The guardian's little helper: microRNAs in the p53 tumor suppressor network. Cancer Res 2007;67:11099-11101.

24. Garzon R, Volinia S, Liu CG, Fernandez-Cymering C, Palumbo T, Pichiorri F, et al. MicroRNA signatures associated with cytogenetics and prognosis in acute myeloid leukemia. Blood 2008;111:3183-3189.

25. Wong TS, Liu XB, Chung-Wai Ho A, Po-Wing Yuen A, Wai-Man Ng R, Ignace Wei W. Identification of pyruvate kinase type M2 as potential oncoprotein in squamous cell carcinoma of tongue through microRNA profiling. Int J Cancer 2008;123:251-257.

EpCAM-Positive Hepatocellular Carcinoma Cells Are Tumor-Initiating Cells With Stem/Progenitor Cell Features

TARO YAMASHITA,* JUNFANG JI,* ANURADHA BUDHU,* MARSHONNA FORGUES,* WEN YANG,‡ HONG–YANG WANG,‡ HULIANG JIA,§ QINGHAI YE,§ LUN–XIU QIN,§ ELAINE WAUTHIER,‖ LOLA M. REID,‖ HIROSHI MINATO,¶ MASAO HONDA,¶ SHUICHI KANEKO,¶ ZHAO–YOU TANG,§ and XIN WEI WANG*

*Liver Carcinogenesis Section, Laboratory of Human Carcinogenesis, Center for Cancer Research, National Cancer Institute, Bethesda, Maryland; ‡International Cooperation Laboratory on Signal Transduction, Eastern Hepatobiliary Surgery Institute, Shanghai, China; §Liver Cancer Institute and Zhongshan Hospital, Fudan University, Shanghai, China; ‖Department of Cell and Molecular Physiology, University of North Carolina School of Medicine, Chapel Hill, North Carolina; and the ¶Liver Disease Center and Kanazawa University Hospital, Kanazawa University, Kanazawa, Japan

Background & Aims: Cancer progression/metastases and embryonic development share many properties including cellular plasticity, dynamic cell motility, and integral interaction with the microenvironment. We hypothesized that the heterogeneous nature of hepatocellular carcinoma (HCC), in part, may be owing to the presence of hepatic cancer cells with stem/progenitor features. **Methods:** Gene expression profiling and immunohistochemistry analyses were used to analyze 235 tumor specimens derived from 2 recently identified HCC subtypes (EpCAM$^+$ α-fetoprotein [AFP$^+$] HCC and EpCAM$^-$ AFP$^-$ HCC). These subtypes differed in their expression of AFP, a molecule produced in the developing embryo, and EpCAM, a cell surface hepatic stem cell marker. Fluorescence-activated cell sorting was used to isolate EpCAM$^+$ HCC cells, which were tested for hepatic stem/progenitor cell properties. **Results:** Gene expression and pathway analyses revealed that the EpCAM$^+$ AFP$^+$ HCC subtype had features of hepatic stem/progenitor cells. Indeed, the fluorescence-activated cell sorting–isolated EpCAM$^+$ HCC cells displayed hepatic cancer stem cell–like traits including the abilities to self-renew and differentiate. Moreover, these cells were capable of initiating highly invasive HCC in nonobese diabetic, severe combined immunodeficient mice. Activation of Wnt/β-catenin signaling enriched the EpCAM$^+$ cell population, whereas RNA interference-based blockage of EpCAM, a Wnt/β-catenin signaling target, attenuated the activities of these cells. **Conclusions:** Taken together, our results suggest that HCC growth and invasiveness is dictated by a subset of EpCAM$^+$ cells, opening a new avenue for HCC cancer cell eradication by targeting Wnt/β-catenin signaling components such as EpCAM.

Tumors originate from normal cells as a result of accumulated genetic/epigenetic changes. Although considered monoclonal in origin, tumor cells are heterogeneous in their morphology, clinical behavior, and mo-lecular profiles.[1,2] Tumor cell heterogeneity has been explained previously by the clonal evolution model[3]; however, recent evidence has suggested that heterogeneity may be owing to derivation from endogenous stem/progenitor cells[4] or de-differentiation of a transformed cell.[5] This hypothesis supports an early proposal that cancers represent "blocked ontogeny"[6] and a derivative that cancers are transformed stem cells.[7] This renaissance of stem cells as targets of malignant transformation has led to realizations about the similarities between cancer cells and normal stem cells in their capacity to self-renew, produce heterogeneous progenies, and limitlessly divide.[8] The cancer stem cell (CSC) (or tumor-initiating cell) concept is that a subset of cancer cells bear stem cell features that are indispensable for a tumor. Accumulating evidence suggests the involvement of CSCs in the perpetuation of various cancers including leukemia, breast cancer, brain cancer, prostate cancer, and colon cancer.[9–13] Experimentally, putative CSCs have been isolated using cell surface markers specific for normal stem cells. Stem cell–like features of CSC have been confirmed by functional in vitro clonogenicity and in vivo tumorigenicity assays. For example, leukemia-initiating cells in nonobese diabetic, severe combined immunodeficient (NOD/SCID) mice are CD34^{++}CD38$^-$.[11] Breast cancer CSCs are CD44$^+$CD24$^{-/low}$ cells, whereas tumor-initiating cells of the brain, colon, and prostate are CD133$^+$.[10,12,13] CSCs are considered more metastatic and drug-/radiation-resistant than non-CSCs in the tumor, and are responsible for cancer relapse. These findings warrant the development of treatment strategies that can specifically eradicate CSCs.[14,15]

Hepatocellular carcinoma (HCC) is the third leading cause of cancer death worldwide.[16] Although the cellular origin of HCC is unclear,[17,18] HCC has heterogeneous pathologies and genetic/genomic profiles,[19] suggesting that HCC can initiate in different cell lineages.[20] The liver is considered as a maturational lineage system similar to that in the bone marrow.[21] Experimental evidence indicates that certain forms of hepatic stem cells (HpSCs), present in human livers of all donor ages, are multipotent and can give rise to hepatoblasts,[22,23] which are, in turn, bipotent progenitor cells that can progress either into hepatocytic or biliary lineages.[22,24] α-fetoprotein (AFP) is one of the earliest markers detected in the liver bud specified from the ventral foregut,[25,26] but its expression has been found only in hepatoblasts and to a lesser extent in committed hepatocytic progenitors, not in later lineages or in normal human HpSC.[22] Recent studies also have indicated that EpCAM is a biomarker for HpSC because it is expressed in HpSCs and hepatoblasts.[22-24]

We recently identified a novel HCC classification system based on EpCAM and AFP status.[27] Gene expression profiles revealed that EpCAM[+] AFP[+] HCC (referred to as *HpSC-HCC*) has progenitor features with poor prognosis, whereas EpCAM[−] AFP[−] HCC (referred to as *mature hepatocyte-like HCC*; MH-HCC) have adult hepatocyte features with good prognosis. Wnt/β-catenin signaling, a critical player for maintaining embryonic stem cells,[28] is activated in EpCAM[+] AFP[+] HCC, and EpCAM is a direct transcriptional target of Wnt/β-catenin signaling.[29] Moreover, EpCAM[+] AFP^{+} HCC cells are more sensitive to β-catenin inhibitors than EpCAM^{−} HCC cells in vitro.[29] Interestingly, a heterogeneous expression of EpCAM and AFP was observed in clinical tissues, a feature that may be attributed to the presence of a subset of CSCs. In this study, we have confirmed that EpCAM^{+} HCC cells are highly invasive and tumorigenic, and have activated Wnt/β-catenin signaling. We also show a crucial role of EpCAM in the maintenance of hepatic CSCs. Our data shed new light on the pathogenesis of HCC and may open new avenues for therapeutic interventions for targeting hepatic CSCs.

Materials and Methods

Clinical Specimens

HCC samples were obtained with informed consent from patients who underwent radical resection at the Liver Cancer Institute of Fudan University, Eastern Hepatobiliary Surgery Institute, and the Liver Disease Center of Kanazawa University Hospital, and the study was approved by the institutional review boards of the respective institutes. The microarray data from clinical specimens are available publicly (GEO accession number, GSE5975).[27] Array data from a total of 156 HCC cases (155 hepatitis B virus [HBV]-positive) corresponding to 2 subtypes of HCC (ie, HpSC-HCC and MH-HCC), were

used to search for HpSC-HCC–associated genes (Supplementary Table 1; see supplementary material online at www.gastrojournal.org). A total of 79 formalin-fixed and paraffin-embedded HCC samples were used for immunohistochemistry (IHC) analyses (Supplementary Table 2; see supplementary material online at www.gastrojournal. org), 56 of which also were used in a recent study.[30] The classification of HpSC-HCC and MH-HCC was based on previously described criteria.[27]

Cell Cultures and Sorting

Human liver cancer cell lines (HuH1 and HuH7) were derived from Health Science Research Resources Bank (JCRB0199 and JCRB0403, respectively) and routinely cultured as previously described.[31] Normal human MHs, provided by the University of Pittsburgh through Liver Tissue Cell Distribution System, were cultured as previously described.[32] Human HpSCs were isolated from fetal livers and cultured in Kubota and Reid's[33] medium as previously described. Wnt10B conditioned medium was prepared as described.[34] Embryonic stem cell culture medium was prepared using Knockout Dulbecco's modified Eagle medium supplemented with 18% of Serum Replacement (Invitrogen, Carlsbad, CA). The pTOP-FLASH and pFOP-FLASH luciferase constructs were described previously.[29] BIO and MeBIO were generous gifts from Ali Brivanlou (The Rockefeller University, New York, NY). For isolating single cell–derived colonies to determine whether heterogeneity is an intrinsic property of EpCAM^{+} cells, HuH1 and HuH7 cells were resuspended and plated as a single cell per well in 96-well plates. A total of 192 single cells were plated successfully. The clones that grew well were selected 2 weeks after seeding and used for immunofluorescence (IF) analysis. The 5-fluorouracil (5-FU) stock (2 mg/mL; Sigma, St Louis, MO), was prepared in distilled water. Fluorescence-activated cell sorting (FACS) and magnetic-activated cell sorting (MACS) analyses were used to isolate EpCAM^{+} HCC cells (Supplementary materials; see supplementary Materials and Methods online at www. gastrojournal.org).

Clonogenicity, Spheroid Formation, Invasion, Quantitative Reverse Transcription–Polymerase Chain Reaction, and IHC Assays

For colony formation assays, 2000 EpCAM[+] or EpCAM^{−} cells were seeded in 6-well plates after FACS. After 10 days of culture, cells were fixed by 100% methanol and stained with methylene blue. For spheroid assays, single-cell suspensions of 1000 EpCAM[+] or EpCAM^{−} cells were seeded in 6-well Ultra-Low Attachment Microplates (Corning, Corning, NY) after FACS. The number of spheroids was measured 14 days after seeding. Invasion assays were performed using BD Bio-Coat Matrigel Matrix Cell Culture Inserts and Control Inserts (BD Biosciences, San Jose, CA) essentially as pre-

viously described.[31] Reverse transcription–polymerase chain reaction and IHC assays are described in detail in the supplementary materials (see supplementary material online at www.gastrojournal.org).

Tumorigenicity in NOD/SCID Mice

Six-week-old NOD/SCID mice (NOD/NCrCRl-*Prkdc*[scid]) were purchased from Charles River (Charles River Laboratories, Inc, Wilmington, MA). The protocol was approved by the National Cancer Institute–Bethesda Animal Care and Use Committee. Cells were suspended in 200 μL of Dulbecco's modified Eagle medium and Matrigel (1:1), and a subcutaneous injection was performed. The size and incidence of subcutaneous tumors were recorded. For histologic evaluation, tumors were formalin-fixed, paraffin-embedded or embedded directly in OCT compound (Sakura Finetek, Torrance, CA) and stored at −80°C.

RNA Interference

A small interfering RNA (siRNA) specific to *TACSTD1* (SI03019667) and a control siRNA (1022076) were designed and synthesized by Qiagen (Qiagen, Valencia, CA). Transfection was performed using Lipofectamine 2000 (Invitrogen), according to the manufacturer's instructions. A total of 200 nmol/L of siRNA duplex was used for each transfection.

Statistical Analyses

The class comparison and gene clustering analyses were performed as previously described.[30] The canonic pathway analysis was performed using Ingenuity Pathways Analysis (v5.5; Ingenuity Systems, Redwood City, CA). The association of HCC subtypes and clinicopathologic characteristics was examined using either the Mann–Whitney U test or the chi-square test. Student t tests were used to compare various test groups assayed by colony formation, spheroid formation, or invasion assays. The Kaplan–Meier survival analysis was performed to compare patient survival or tumorigenicity.

Results

A Poor Prognostic HCC Subtype With Molecular Features of HpSC

We re-evaluated the gene expression profiles that were uniquely associated with 2 recently identified prognostic subtypes of HCC (ie, HpSC-HCC and MH-HCC), using a publicly available microarray dataset of 156 HCC cases (GEO accession number: GSE5975). Sixty cases were defined as HpSC-HCC with a poor prognosis and 96 cases were defined as MH-HCC with a good prognosis, based on EpCAM and AFP status.[27] A class-comparison analysis with univariate t tests and a global permutation test (1000×) yielded 793 genes that were expressed differentially between HpSC-HCC and MH-HCC ($P < .001$). Hierarchical cluster analyses revealed 2 main gene clus-

ters that were up-regulated (cluster A; 455 genes) or down-regulated (cluster B; 338 genes) in HpSC-HCC (Figure 1A). Pathway analysis indicated that the enriched genes in cluster A were associated significantly with known stem cell signaling pathways such as transforming growth factor-β, Wnt/β-catenin, PI3K/Akt, and integrin ($P < .01$) (Figure 1B). In contrast, genes in cluster B were associated significantly with mature hepatocyte functions such as xenobiotic metabolism, complement system, and coagulation system ($P < .01$). Noticeably, known HpSC markers such as *KRT19* (CK19), *TACSTD1* (EpCAM), *AFP*, *DKK1*, *DLK1*, and *PROM1* (CD133) were up-regulated significantly in HpSC-HCC, whereas known liver maturation markers such as *UGT2B7* and *CYP3A4* were expressed more abundantly in MH-HCC (Figure 1C and Supplementary Tables 3 and 4; see supplementary material online at www.gastrojournal.org). Kaplan–Meier survival analysis revealed that HpSC-HCC patients had a significantly shorter survival than MH-HCC patients ($P = .036$) (Figure 1D). Consistently, HpSC-HCC patients had a high frequency of macroscopic and microscopic portal vein invasion (Figure 1E).

However, IHC analyses of an additional 79 HCC cases revealed that among 24 HpSC-HCC cases, EpCAM staining was very heterogeneous with a mixture of EpCAM+ and EpCAM− tumor cells in each tumor (Figure 1F, *left panel*). Noticeably, many of the EpCAM+ tumor cells were located at the invasion border zones and often were disseminated at the invasive front (*black arrows*). IF analysis revealed that HCC cells located at the invasive front co-expressed EpCAM, CK19, and AFP (Figure 1F, *right panels*). Noticeably, HpSC-HCC patients were significantly younger than MH-HCC patients (Supplementary Tables 1 and 2; see supplementary material online at www.gastrojournal.org). Enrichment of EpCAM+ AFP+ tumor cells at the tumor-invasive front suggested their involvement in HCC invasion and metastasis.

Isolation and Characterization of EpCAM+ Cells in HCC

The results described earlier suggest that HpSC-HCC may be organized in a hierarchical fashion in which EpCAM+ tumor cells act as stem-like cells with an ability to differentiate into EpCAM− tumor cells. To test this hypothesis, we first evaluated the expression pattern of 7 hepatic stem/maturation markers (EpCAM, CD133, CD90, CK19, Vimentin, Hep-Par1, and β-catenin) in 6 HCC cell lines (Figure 2A). All 3 AFP+ cell lines (HuH1, HuH7, and Hep3B) expressed EpCAM, CD133, and cytoplasmic/nuclear β-catenin, whereas the other 3 AFP− cell lines (SK-Hep-1, HLE, and HLF) did not, consistent with the microarray data. Interestingly, AFP+ cell lines had no CD90+ cell population, which recently was identified as hepatic CSCs,[35] whereas AFP− cell lines had such a population. Consistent with the IF data, FACS analysis showed that AFP+ cell lines had a subpopulation of